JOURNAL OF CHEMICAL INFORMATION AND MODELING

Article

pubs.acs.org/jcim

Screen3D: A Novel Fully Flexible High-Throughput Shape-Similarity Search Method

Adrián Kalászi,* Dániel Szisz, Gábor Imre, and Tímea Polgár*

ChemAxon Ltd., Graphisoft park, Zahony u. 7, Budapest, Hungary, 1037

Supporting Information

ABSTRACT: 3D shape- or volume-based virtual screening is a broadly used approach in drug discovery. In recent years a large number of publications have appeared in which these tools were compared not only to competitive methods but to docking studies as well. Studies often showed that the effectiveness of docking could be highly variable due to a large number of possible confounding factors, while ligand-based, shape-based approaches were more consistent. Here, we describe a novel, fully flexible shape-based virtual screening algorithm that does not require previous 3D conformation or conformer generation. Due to its solid consistency it can easily be used on desktop computers by non-expert scientists. The algorithm is demonstrated in a study for the investigation of β-secretase inhibitors and benchmarked on the Directory of Useful Decoys data set.

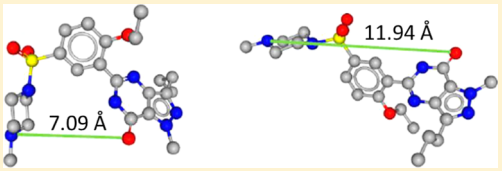

INTRODUCTION

Virtual screening (VS) has become an important part of the armamentarium of modern drug discovery.[1] The most important drive to use virtual screening has arisen from increased pressure to reduce the costs of lead discovery.[2] Given the known costs involved in experimental high-throughput screening (HTS), virtual screening has been frequently applied to reduce the number of compounds going into HTS. There are two fundamental types of virtual screening systems: structure-based approaches, such as docking and de novo design, can be used when the 3D structure of the protein target is available; and ligand-based approaches that are applicable in the absence of such structural information.[2,3] Scientific literature discusses both methods thoroughly; therefore, we only briefly discuss ligand-based methods as an introduction to our novel shape-based algorithm.

Ligand-based methods involve 2D (2-dimensional) and 3D (3-dimensional) similarity searches.[2,4] A wide variety of 2D similarity methods were developed over the past decades,[5,6] such as substructure-based similarity approaches that calculate similarity values based on the Maximum Common Substructure (MCS) overlap.[7] This approach can provide substructure matching between the query and the computational hits, thus it offers chemical insights into the relationship between molecular structure and biological activity (SAR). Fingerprint-based (FP) similarity approaches first determine the identical fragments of the query and the database molecules and calculate the binary fingerprint patterns.[8] Finally the similarity values based on the matches of the fingerprint patterns are calculated. Topological descriptors and atom-pair descriptors can also be used for molecular similarity calculations.[9] Although the efficiency of 2D similarity methods has already been demonstrated, the often cited limitations of these and other 2D approaches include their limited ability for scaffold hopping and the lack of structural insights.[9−14] To address these issues, 3D similarity methods have been developed, which can also provide molecular alignments helping pharmacophore hypothesis generation during lead optimization.[15−20] In contrast to the 2D search methods, the structural graph of the molecules does not require a match of the two molecules in the 3D search methods. 3D similarity searching falls into categories of pharmacophore-based and shape- or volume-based methods. While pharmacophore-based queries give topological and geometric constraints for the search, the latter utilizes 3D information including shape, volume, or electrostatic properties. There are various commercial software packages offering 3D similarity searches, just to mention ROCS,[21] FlexS,[22] or Phase Shape.[23] 3D similarity methods face the challenge of the composition of an easily computable and chemically meaningful mathematical function that has the ability to represent spatial arrangements of atoms. The definition of molecular similarity is typically resolved via maximal molecular volume between molecules. This must be realized by a fast and robust molecular alignment algorithm that can also handle molecular flexibility. Most tools perform a time-consuming discrete sampling of the conformational space. An ideal overcome can be a continuous way of sampling the conformational space by incorporating the rotational degrees of freedom in the object function.

In this paper we publish a novel algorithm, Screen3D, that performs shape-based 3D similarity searches on large databases in a fully automatic way without the need of preliminary conformer and conformation generation. First, we demonstrate its best practices emphasizing its advantages and limitations in a virtual screening study. As a focus of our virtual screening study we selected β-secretase (BACE1); BACE1 is the most popular aspartic protease target, and one of the richest pools for pharmaceutical research aiming to find potential drug

Received: October 24, 2013
Published: February 25, 2014

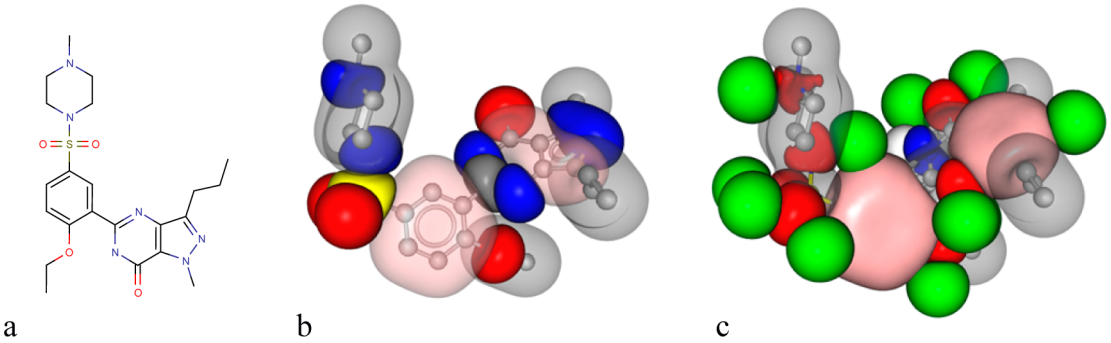

Figure 1. a: Structure of Sildenafil, b: van der Waals volume colored by ChemAxon's extended atom types (pink: aromatic carbon, gray: sp2 and sp3 carbons, blue: sp2 sp3 and aromatic nitrogen, yellow: sulfur, red: sp2, sp3 oxygen), c: van der Waals volume colored by pharmacophore types (pink: aromatic, red: H-bond acceptor atom, blue: H-bond donor atom, white: H atoms, green: acceptor regions).

candidates for Alzheimer's disease treatment. Despite numerous attempts only HIV protease and renin inhibitors were brought to the market. Nevertheless, several inhibitors targeting renin, BACE1 and γ-secretase are in clinical or preclinical phase, and some others are discussed as potential drug targets. Since BACE1 has already been investigated in some of our previous studies,[14,24,25] we extended our studies with Screen3D. Second, a head-to-head comparison to Screen2D is shown, and the performance of Screen3D is demonstrated in contrast to other competitive virtual screening methods.[26,27]

METHODS

In this section we first describe the novel Screen3D algorithm with setups demonstrating its best practices. Then we detail the screening data sets used for virtual screening studies. The settings applied for the comparative virtual screening studies including setups for Screen2D similarity searches, Gold docking protocols, and Screen3D similarity searches on Venkatraman's and Giganti's data sets[26,27] are provided. We also discuss how the virtual screening runs were analyzed and compared.[28]

Screen3D. *Preprocess Structures.* The input molecules are processed in the following way: the valence errors are checked and fixed, the Kekule form is converted to aromatic form, the largest fragment is kept, and explicit hydrogen atoms are removed using the ChemAxon's Standardizer[29] module. The 3D coordinates are used from the input structure if available or generated by ChemAxon's Generate3D[29] tool otherwise. In the subsequent step atomic types are assigned to atoms of the preprocessed molecule. Available type sets are either "extended" atom types calculated by the in-house implementation of Dreiding[30] force field or pharmacophrore types[29] (Figure 1).

Molecular Alignment. The alignment algorithm overlays two preprocessed molecules and returns an overlay pose and a shape similarity score. Conformation of both molecules can be kept either rigid or flexible during the alignment process. If a molecule is initialized as rigid, only the translational and rotational movements are allowed during the alignment. Alternatively, if the molecule is treated flexible, dihedral angles of rotatable bonds are also allowed to change during the overlay process to maximize the shape intersection of the two structures.

Molecular shape overlay is done via two algorithms (Shape and Match); both comprise of two major parts: Step 1 generates diverse orientations and conformations, and step 2 performs gradient based numerical optimization starting from the orientations/conformations generated in step 1. As step 2 is identical in both algorithms it is described first.

In step 2, numerical optimization is done by an optimizer that uses a multidimensional subspace search algorithm (MDS), an enhanced version of the conjugate gradient (CG) search. The MDS search algorithm assumes a linear relation between the force and coordinate changes. The search algorithm builds a subspace using N previous points that is the force and step difference vectors. These are used to build an NxN subspace Hessian matrix that represents the linear connection. This matrix is then used to solve the dX H = dF equation, that is we try to minimize the force in the subspace. The residual force component is then used for an outer CG (or simple SD) step.[31]

Scoring Function of Molecular Shape Intersection. The molecular shape is approximated with atom centered spheres with the van der Waals radius. According to the inclusion-exclusion principle, to calculate the accurate and homogeneous molecular shape numerous shape correction terms should be included to compensate the effect of the multiple intersections. The number of correction terms however scales exponentially with the atom count, for example $\sim 10^{15}$ correction terms are required for an average drug structure with 50 heavy atoms. To make shape overlay evaluation computationally tractable we consider only the first order correction (eq 1).

$$V_A = \sum_{i=1}^{n} |A_i| - \sum_{1 \le i \le j \le n} |A_i \cap A_j| \approx \sum_{i=1}^{n} |A_i| - \sum_{k=1}^{m} |A'_k| \quad (1)$$

Equation 1 denotes Shape overlay, where A_i is the i^{th} atom centered sphere contribution to the molecular volume (V_A), and n is the number of atoms. To further reduce the number of intersection terms to calculate, we include only those, which are between atoms connected with a chemical bond (A'). We introduced two options for describing the shape quality: "normal" with only the atomic contributions and the "accurate" mode when shape corrections terms are also included (eq 2).

$$\begin{aligned} F_{AB} = & \sum_i \sum_j w(t_i, t_j)|A_i \cap B_j| - \sum_k \sum_j w(t_k, t_j)|A'_k \cap B_j| \\ & - \sum_i \sum_l w(t_i, t_l)|A_i \cap B'_l| \\ & + \sum_k \sum_l w(t_k, t_l)|A'_k \cap B'_l| \end{aligned} \quad (2)$$

Equation 2 denotes the Shape intersection function (Screen3D score) between two molecules (V_A and V_B), where atoms of molecule A and B are labeled with A_i and B_j, respectively, and $w(t_i,t_j)$ is a real valued weight factor for atom types t_i and t_j. The current defaults for w are 1 for identical and 0 for different atom

dx.doi.org/10.1021/ci400620f | J. Chem. Inf. Model. 2014, 54, 1036−1049

types; however, optionally any custom weight factor can be introduced for the desired atom types enabling manual fine-tuning of the alignment scoring function, e.g.: (sp3 carbon − aromatic carbon: 0.3).

The calculation of volume intersection for two spheres $|A_i \cap B_j|$ is analytically feasible; however, this is not a trivial task for triple and quadruple intersections as in $|A'_k \cap B_j|$, $|A_i \cap B'_l|$, and $|A'_k \cap B'_l|$. To solve this issue we substitute each correction term of the individual molecules (like A' and B') with a sphere, that has the same volume as the correction term, and with the origin in the center of mass of the two atomic spheres in question. As a result the calculation of F_{AB} gets back to the calculation of the sum of the volume contributions (ϑ) (eq 3).

$$F_{AB} = \sum_i \vartheta(r_i) \approx \sum_i \sigma(r_i) \tag{3}$$

Equation 3 denotes the sum of the volume contributions calculated for intersections, where r_i is the distance of the centers the two spheres. $\vartheta(r_i)$ has discontinuity in the second derivate, so it cannot be used directly in optimization; hence we approximated this function with a cubic spline (σ), which operates well in optimization (Figure 2).

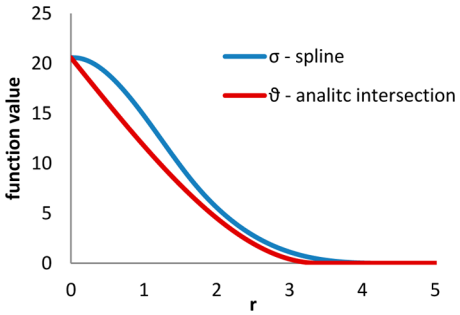

Figure 2. Volume of the intersection of the two spheres as a function of the distance of origins. $\vartheta(r)$ (red) and approximated with a cubic spline (blue).

Further property of spline function can be exploited to speed up calculation as both the function value, the gradient and second derivate vanish after a given cutoff. A Tanimoto-like normalized value of F_{AB} can also be calculated using the equation $T_{AB} = F_{AB}/(F_{AA}+F_{BB}-F_{AB})$ (Tanimoto similarity score).

The degrees of freedoms (DFs) during the MDS optimization of F_{AB} are the rigid body translation and rotation. The representation of spatial rotation utilizes *unit* quaternions. Unit quaternions have much better convergence properties than Euler-angles and have the advantage of being able to avoid the *gimbal lock* problem, which loses one degree of freedom in the rotational space.

However, when the unit quaternions are used, the search space is constrained; as in each optimization step a normalized 4-vector has to be found. One possible solution is to incorporate a *penalty* term in the object function that forces the norm of the quaternion to be 1. We have chosen an alternative approach by exploiting the special mathematical property of the space of unit quaternions. Using the exponential function $exp(q)$ defined for quaternions (that is a generalization of the exponential function for complex numbers) it is possible to project the actual step done by the optimizer in the 4-vector space (representing quaternions) onto the sphere of unit quternions. This exponential was incorporated in the analytical calculation of the rotational gradient. With this approach it is possible to keep the pure analytical formula of the derivatives, avoid gimbal lock problems, and maintain good convergence properties in terms of the rotational degree of freedom.

When requested, the number of DFs can be further extended by the number of rotatable bonds, tweaking them in a continuous manner during the optimization (directed tweak).[32]

Orientation Algorithms. As the numerical optimization finds a local solution to F_{AB}, we sample the domain of F_{AB} and start the optimization process from multiple starting points. We have implemented two radically different algorithms to generate diverse orientations and conformations for the shape optimization process above.

Orientation Algorithms, Shape Method. The process starts with the generation of n random conformations if the molecule is treated flexible: the rotatable bonds are tweaked by random values. The value of n depends on the number of rotatable bonds in the molecule; that is typically 3 for drug-like structures. Then for every conformation 2, 3, or 4 anchor atoms are selected based on a topological analysis of the molecule. These anchor atoms are typically selected along the longest open chain of the molecular graph, typically the first and last atoms. The two molecules are aligned according to these anchor atoms in all combinations using JQuatFit, the ChemAxon's in-house implementation of the Kabsch's algorithm.[33] These two steps usually generate 30 to 60 approximately aligned structure pairs. An optimization is executed for each pair of structures using an F_{AB}, which has only some selected atoms/features included only. Included features are the following: noncarbon heavy atoms, aliphatic and aromatic ring centers. This process results in 30−60 orientations and alignment scores, out of which the best with the highest score is optimized with the all-atom F_{AB}.[34,35]

Orientation Algorithms, Match Method. This type of orientation algorithm needs an extra preprocessing step: minimum and maximum intramolecular distances between the selected subset of atom pairs are calculated. This calculation is performed, using the numerical optimization method described above, on a function that is comprised of a constraint term for the atomic pair in question and potential energy terms describing the atomic repulsion. The DFs in this case are the rotatable bonds only (Figure 3). The selected atoms include

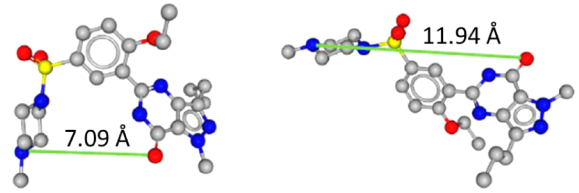

Figure 3. Minimum and maximum intramolecular distances between a selected atom pair in Sildenafil.

non-carbon atoms, aromatic ring centers, and aliphatic ring centers. It is worth noting that distance range generation is equivalent to a continuous conformational sampling.

The purpose of the following algorithm is to identify atom−atom mappings between the two molecules to align. First, for every selected atom of both molecules an atomic environment histogram is generated (Figure 4). These histograms describe the environment of the current atom from atom type and

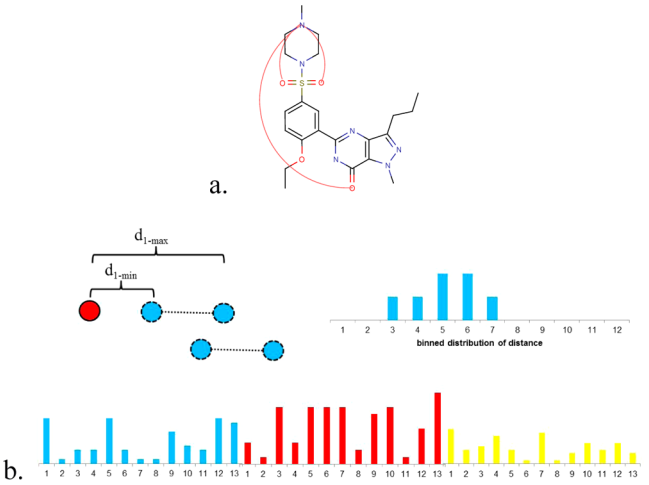

Figure 4. a: Example distance range pairs in Sildenafil between one selected sp3 N atom and all the sp2 O atoms. b: The red circle represents the selected sp3 N atom, the blue ones per line, one oxygen atom. The $d_{1\text{-min}}$ and $d_{1\text{-max}}$ are the minimum and maximum intermolecular distances respectively. A binned distribution of distance ranges is generated between the specific sp3 N atom and all the sp2 O atoms. A set of such histograms is assigned to that specific sp3N: on the figure a schematic set of distance range distributions are shown; for all sp2 O (blue), for all aromatic carbons (red), and for all aromatic nitrogen atoms (yellow). The histogram does not represent the actual real distance ranges in the molecule; they are for demonstration purposes only.

conformational perspective. A similarity of two atoms by their environment is calculated using the normalized histogram similarity measure (eq 4).

$$\varphi(A_i, B_j) = \frac{\sum_{k=1}^{n} \min(h_k(A_i), h_k(B_j))}{\sum_{k=1}^{n} \max(h_k(A_i), h_k(B_j))} \quad (4)$$

Equation 4 denotes normalized histogram similarity measure, where A_i and B_j are atoms from the different molecules, and h_k represents the k^{th} histogram height. The position of a single histogram bar (k) is defined by its assigned atom type and the distance. When two atoms are assigned, different histograms are compared, the $h_k(A_i)$ and $h_k(B_j)$ will still represent the same type of environment.

Molecular similarity (eq 5) S between the two structures to align is defined as the sum of the atomic similarities.

$$S_{AB} = \sum_i \varphi(A_i, p(A_i)) \quad (5)$$

Equation 5 denotes molecular similarity, and $p(A_i)$ stands for the mapping of A_i.

The mapping algorithm, which uses backtracking, returns the n different atom−atom mapping set for the n largest S_{AB}. These mappings are then used as an input for the in-house developed flexible-Kabsch hybrid alignment. This type of alignment uses stepwise numerical optimization in the dihedral angle space to minimize the rmsd of the atoms of the mapping; additionally in every step it also performs a one step overlay to minimize the same rmsd according to translation and rotation using the Kabsch algorithm.[33] This kind of alignment treats the conformation in continuous space and at the same time it keeps the speed and robustness of the Kabsch approach. As a result the orientation and conformation of the molecules is changed to maximize the rmsd on the atom mapping. These structures are used as an input for the alignment score (F_{AB}) optimization as described above.

Setups for Screen3D Best Practices. Screen3D calculations first were executed with the following settings: first, screens were performed with the crystallographic conformation of queries and second with flexible queries. The molecules in the target database were always kept flexible. Shape and Match methods were both studied with these parameters. These setups were repeated for both screening library compilations resulting in eighty screens (Supporting Information).

Second, we included further parameters: the number of initial conformations, which was increased from two (default) to five; atom typing, which was changed to pharmacophore type from ChemAxon's extended atom types (default); the accuracy of molecular alignments, fast, normal (default) and accurate alignment options were studied. These parameters were investigated using three selected query structures in twenty-one runs (Supporting Information).

Data Sets. Two screening libraries were compiled to perform the virtual screening studies. Our first screening library includes a subset of Directory of Useful Decoys (DUD)[36,37] as inactive molecules; decoys for HIV protease (2038 molecules), HSP-90 (979 molecules), PPAR-γ (3127 molecules), and ADA (927 molecules) were selected. The molecules were standardized by ChemAxon's Standardizer, and the structures were checked for atom type or bond errors by ChemAxon's Structure checker.[29] 4980 of 7071 molecules having molecular weight in the range of 300 and 620 Da were used for virtual screening, the most similar molecular weight range to the actives. This ad hoc subset was compiled for comparison purposes.

The second set of decoys was compiled from DUD-E,[38] β-secretase (BACE1) set of 18221 molecules. 4980 molecules were selected by Instant JChem's diverse set selection method.[29] This method was implemented as a groovy script and applied a maximal Tanimoto similarity index of 0.7, which was calculated by ChemAxon's Chemical Fingerprint.[29]

We compiled one active set by diverse selection of 20 BACE inhibitors from the 197 available ligands found in the PDB database. The ligands were extracted from the following X-ray structures: 4HA5,[39] 3INF,[40] 3S2O,[41] 2OHU,[42] 3RSV,[43] 3ZKI,[44] 4I0G,[45] 3INH,[40] 4ACU,[46] 4H3I,[39] 4AZY,[47] 2WJO,[46] 3PI5,[48] 4DUS,[49] 3DUY,[49] 3UDQ,[49] 3FKT,[53] 3K5F,[51] 4D83,[52] and 3IVI[53] (Figure 5). The diverse selection was done by JKlustor 6.0[29] using ECFP6 and a maximal Tanimoto similarity threshold of 0.7. Ligand structures were visually inspected and corrected if necessary. The two final screening libraries were comprised of the active set (20 molecules) and the two different inactive sets (4980 molecules), which were stored as sd files. The molecules were treated neutral.[50] The final two screening libraries of 5000 compounds had an active content of 0.4% that mimics real-life screening situations.

For the shape (Screen3D) and fingerprint similarity (Screen2D) searches the following ten ligands manually extracted from the PDB database were used as query molecules: 2VIJ,[55] 2ZJM,[54] 3IND,[56] 3L38,[57] 3L3A,[57] 3L5C,[58] 3LPI,[59] 3MSK,[60] 3RTN,[43] and 3RVI[43] (Figure 6). Ligand structures were visually inspected and corrected if necessary. 3D coordinates of these ligands were stored intact for rigid queries with Screen3D runs. All the molecules were treated neutral.

Screen3D's performance was also shown using the data set in the publication of Venkatraman et al.[26] and Giganti et al.[27] Venkatraman applied the DUD Release 2 data set; for each of

dx.doi.org/10.1021/ci400620f | J. Chem. Inf. Model. 2014, 54, 1036−1049

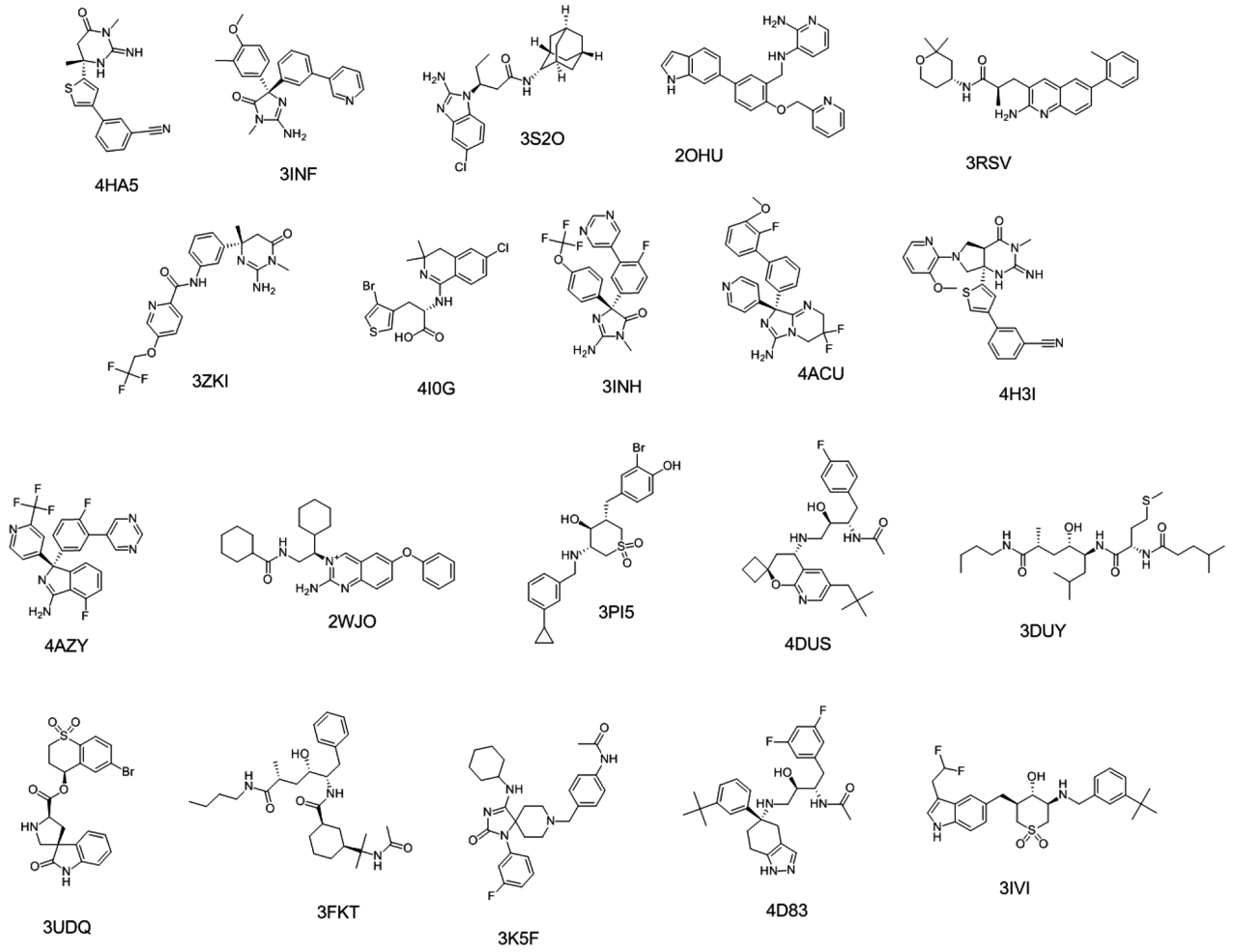

Figure 5. Active molecules added to the decoys comprising screening library.

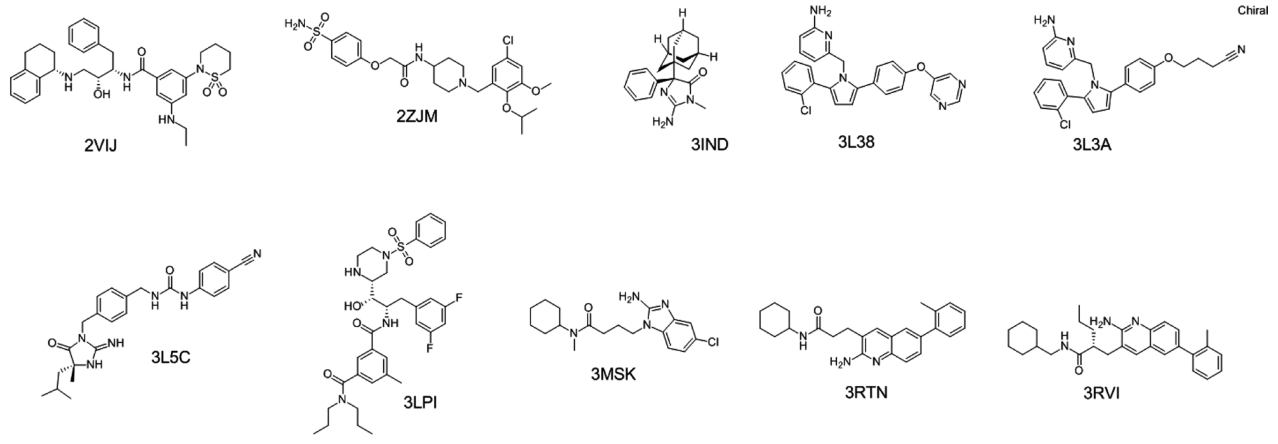

Figure 6. Query molecules used for similarity (Screen2D) and shape-based (Screen3D) screening.

the 40 targets in the data set, the known actives and the target-specific decoys were used. For each target, the crystallographic control ligand conformation provided by Huang et al.[33] was used as the query. DUD structures were used without modification in order to perform a fair comparison. Giganti et al. selected the subset of 11 libraries of DUD Release 2 (ADA, CDK2, DHFR, ER, FXA, HIVRT, NA, P38, THR, TK, TRP) according to their presence in the literature for benchmarking.

Comparative Virtual Screening. *Screen2D.* Similarity searches were executed by the command line toolkit of ChemAxon's Screen2D program.[29] Extended connectivity fingerprints[29] (ECFP6) and pharmacophore fingerprints[29]were were applied with Tanimoto metric on two screening data sets. Enrichments factors[28] and BEDROC(20) values were computed based on the computed Tanimoto similarities. Forty search runs were executed applying the two fingerprints,

dx.doi.org/10.1021/ci400620f | J. Chem. Inf. Model. 2014, 54, 1036−1049

ten queries, and two screening data sets (Supporting Information).

Docking Protocol. Protein Preparation. Enrichment studies were performed on ligand-bound structures of β-secretase. 2VIJ, 2ZJM, 3IND, 3L3A, 3L5C, and 3RTN X-ray structures were selected for docking studies. These are the same X-ray structures of which ligands were used as query molecules for shape- and fingerprint similarity searches. The protein coordinates were used intact, without any minimization. The protonation scheme of the catalytic aspartate residues was as follows: Asp32 protonated and Asp228 ionized as determined in our previous publications.[24,25] The active site was defined as the collection of residues within 6 Å of the bound inhibitor (Figure 7). The bound inhibitor was not included in the docking run. All water molecules were removed from X-ray structures.

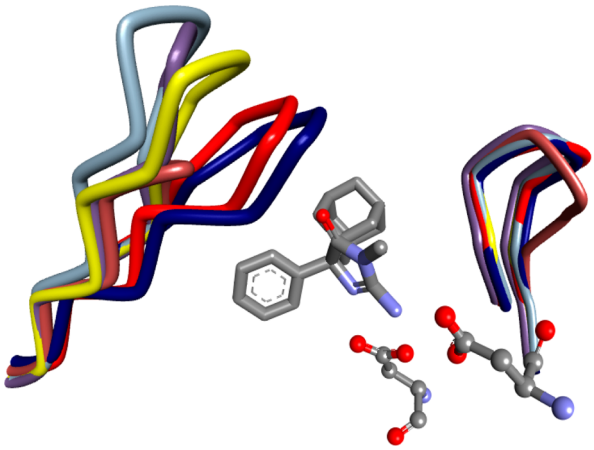

Figure 7. Active site of the BACE1 structures highlighting FLAP (68–74) and 10s loop (9–14) conformation with a ligand of 3IND. Catalytic Asp residues are also highlighted.

GOLD Settings. Standard parameters of Gold 5.1 were used to dock the libraries described above. Gold uses a mol2 file format with explicit hydrogen atoms for proteins. The top-ranked pose, according to the CHEMPLP and Goldscore, was saved for further postprocessing with in-house scripts to rank compounds by decreasing docking scores.[61]

Screening on Venkatraman's and Giganti's data set. The calculations on the same data sets were repeated using Screen3D and Screen2D (Chemical fingerprint, ECFP4). Screen3D was run with flexible and rigid query settings and with Shape and Match algorithms. Screen3D and Tanimoto scores were used for EF and AUC(100%) calculations.

Screening Results Evaluation. *Performance Metrics.* We report the enrichment factor for the top 1% of the database (EF(1%)) and the Boltzmann-enhanced discrimination of the receiver operating characteristic (BEDROC). We use $\alpha = 20$ for the BEDROC calculations, which corresponds to 80% of the BEDROC score accounted for the top 8% of the database screen. Both EF(1%) and BEDROC ($\alpha = 20$) have the desirable characteristic that they emphasize the early part of the receiver operating characteristic (ROC) curve, which is important for applications where only the early part of a database screen is selected for experimental testing.[28]

The Area Under the Curve (AUC) of a ROC plot is also reported for comparison with the work of Venkatraman et al.[26] The AUC is calculated for the whole ROC curve (AUC(100%)).

RESULTS AND DISCUSSION

To show the best practices of Screen3D we first demonstrated the effectiveness of Screen3D, its dependency on the query structures, and the screening libraries (BACE1-DUD, BACE1-DUD-E). Additional Screen3D parameters were investigated on selected Screen3D runs.

Second, we performed a comparative virtual screening study that started with the comparison of Screen2D fingerprint similarity method to Screen3D. Docking calculations were also shown in contrast to selected Screen3D searches. Finally, we compared the performance of Screen3D to several already published virtual screening studies.

Best Practices for Screen3D. *Virtual Screens on BACE1-DUD Data Set.* Maximal EF(1%) of 20 and BEDROC(20) of 0.32 were achieved when crystallized (rigid) query 3MSK was applied for screening with the Shape algorithm, and hits were ranked by the Screen3D similarity score (Figure 8). Shape and Match methods showed comparable performance in terms of EF(1%) and BEDROC(20) values; however, the Shape algorithm provided adequate results for both ranking score. The initialization of the Match algorithm for a rigid query can lead to limited performance because only one conformation is considered during the Tanimoto range histogram calculation Comparing the results given by the ten query molecules, query 3IND, 3MSK, 3RTN, and 3RVI provided the best EF(1%) and BEDROC(20) values independently on the method and on the similarity scores (see the Supporting Information for a full table of EF(1%) and BEDROC(20) values). Query 3RTN and query 3RVI are very similar molecules and showed very similar results as expected, underlining that the algorithm provides consistent and reproducible results. The remaining query (2VIJ, 2ZJM, 3L38, 3L3A, 3L5C, 3LPI) molecules resulted in very poor EF(1%) or BEDROC(20) values; only application of the Tanimoto score ranked 3 (Match), 1 (Shape), and 1 (Shape) actives in the top 1% for 2VIJ, 3L38, and 3LPI queries, respectively. The four best query molecules (3IND, 3MSK, 3RTN, and 3RVI) could retrieve seven out of the twenty actives in the top 1% of the ranked databases (50 molecules) leading to a hit rate of 3.5% (7/200), which is significantly higher than the typical hit rate for an HTS.

When treating the query molecules flexible, the Match algorithm lead to the best EF(1%) of 30 and BEDROC(20) of 0.35 for query 3MSK with the application of Screen3D similarity score. The Match algorithm outperformed the Shape algorithm possibly due to the improved histogram Tanimoto filtering performance that lead to better alignments. It reveals the advantage of the algorithm that initial crystallized conformation is not necessarily needed to find possible binding conformations. Results showed little variations in terms of EF(1%) and BEDROC(20) values for Tanimoto similarity and Screen3D score. 3IND, 3MSK, 3RTN, and 3RVI selected active molecules out of the decoys the best independently on the method and score. The rest of the query molecules retrieved either no actives or maximum two. The four best query molecules (3IND, 3MSK, 3RTN, and 3RVI) resulted in a hit rate of 5%; they retrieved 10 molecules altogether in the top 1% of the ranked databases (10/200).

After a head to head comparison of hits found by rigid and flexibly queries, flexible queries retrieved new hits compared to rigid query runs. In summary, results seemed to be more

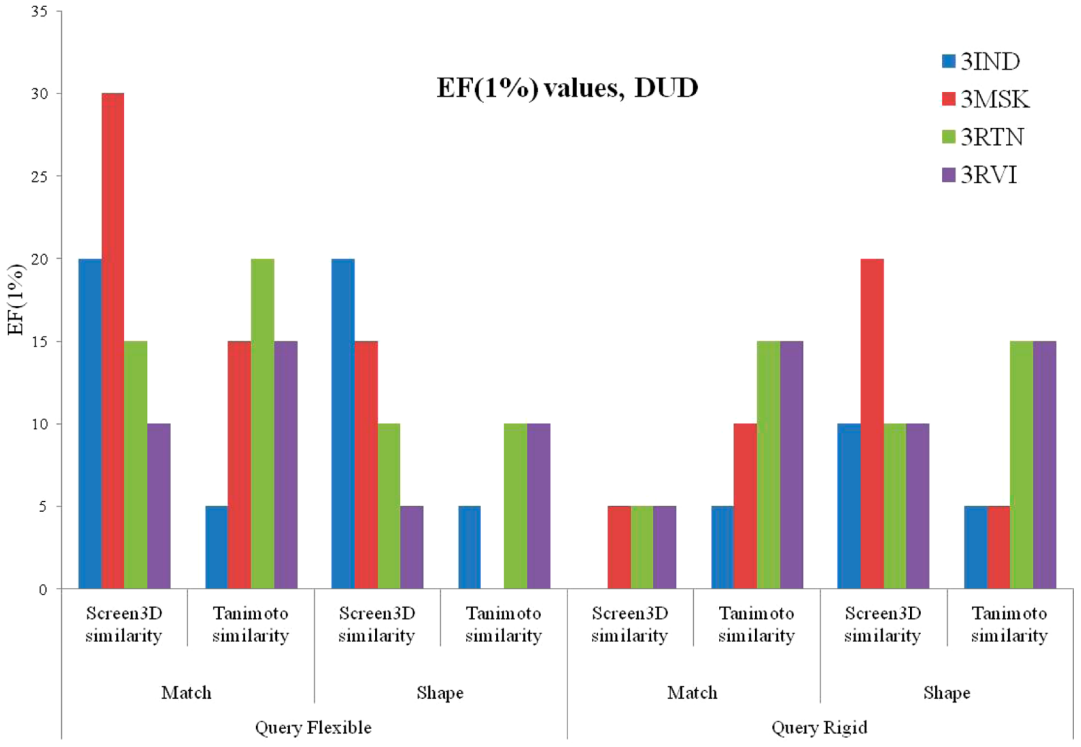

Figure 8. EF(1%) values calculated using 3IND, 3MSK, 3RTN, and 3RVI query structures on the DUD data set. Screen3D similarity stands for F_{AB} and Tanimoto similarity for T_{AB} as defined above.

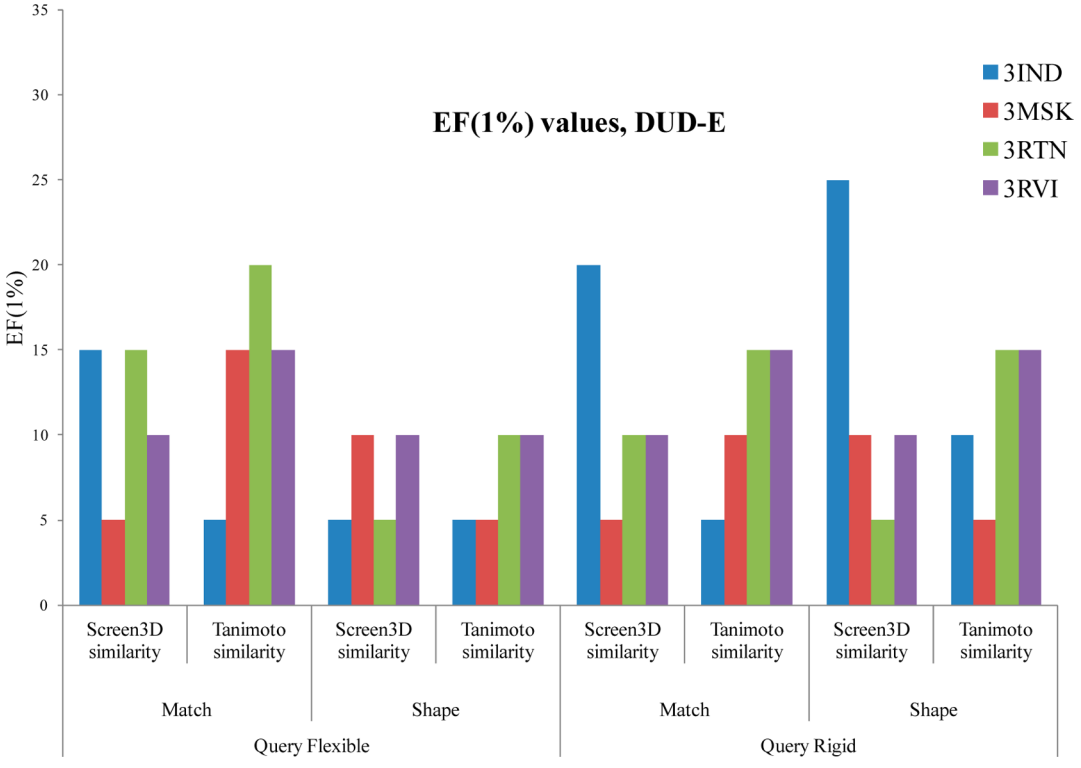

Figure 9. EF(1%) values calculated using 3IND, 3MSK, 3RTN, and 3RVI query structures on the BACE1-DUD-E data set. Screen3D similarity stands for F_{AB} and Tanimoto similarity for T_{AB} as defined above.

dependent on the query structures than on the various methods highlighting the consistency of the computations and the importance of the previous knowledge about the target protein and its ligands.

Virtual Screens on the BACE1-DUD-E Data Set. The Screen3D runs discussed above were repeated on the second screening data set compiled of DUD-E to demonstrate how a different decoy set affects its performance (Figure 9). For rigid query runs the best EF(1%) was 25 (BEDROC(20) = 0.35)

dx.doi.org/10.1021/ci400620f | J. Chem. Inf. Model. 2014, 54, 1036−1049

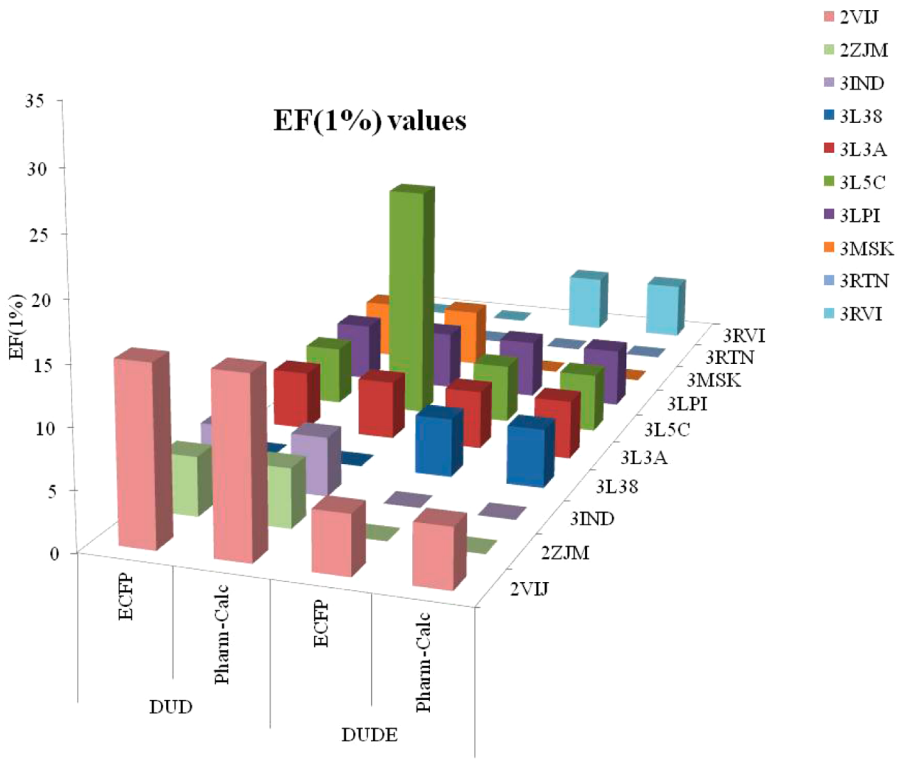

Figure 10. EF(1%) values calculated using 3IND, 3MSK, 3RTN, 3RVI, 2VIJ, and 3L5C query structures on the DUD data set. The runs were executed by the Screen2D program package.

when screening with the Shape method, using query 3IND and ranking by Screen3D similarity score. The Shape algorithm performed similarly to Match. 3IND, 3MSK, 3RTN, and 3RVI provided the best EF(1%) and BEDROC(20) values, similar to the runs on the DUD data set. The rest of the queries resulted in poor results (see the Supporting Information). It is worth noting that query 2VIJ also retrieved active molecules unlikely to the virtual screens on DUD data set. The best hit in the top 1% of the ranked databases rate was 4% (8/200) given by 3IND, 3MSK, 3RTN, and 3RVI query structures.

The application of flexible query structures resulted in the best EFs(1%) of 20 and BEDROC(20) of 0.20 using the Match algorithm and the Tanimoto similarity score. The Match algorithm outperformed the Shape algorithm similarly to the calculations performed against the DUD screening data set. Query structures, 3IND 3MSK, 3RTN, and 3RVI, performed the best identically to that of the DUD data set. The rest of the queries resulted in poor results (see the Supporting Information). The best hit rate in the top 1% of the ranked databases was 4% (8/200) given by 3IND, 3MSK, 3RTN, and 3RVI query structures.

Screen3D searches on DUD and DUD-E screening data sets demonstrated minor differences in EF(1%) that highlights the consistency and independency of the performance on the screening database, when identical active molecules are searched for from various and independent decoy sets. Two independent decoy sets were compiled; the first DUD set was made in an ad hoc way, while the second DUD-E set was a specific selection for BACE1. Our first intention was to test the method on two independent data sets that first of all provide information on the screening library dependence; the second goal was to show how Screen3D operates when the rate of false negatives are unknown. ChemAxon's Chemical fingerprint similarity between the active and inactive molecules had a Tanimoto similarity lower than 0.7 (see the Supporting Information for similarity histograms). Moreover, Screen3D showed insignificant dependence on the query flexibility, on the algorithm applied (Shape, Match), and on the scores. These calculations also revealed that the performance of Screen3D is more dependent on the query structures than on the actual screening parameters. Therefore Screen3D offers an effective way to perform virtual screening studies in the absence of crystallographic information with several setups for computational non-experts. These preliminary results also drew attention to the necessity of thorough knowledge of the target biology.

Evaluation of Additional Screen3D Options. To demonstrate if further parameters available in Screen3D influence the search performance (see the Supporting Information for results), we selected flexible queries and the DUD screening data set (Supporting Information). We restricted ourselves to report only a few cases to report their influence if there is. One flexible query (2VIJ), which resulted in poor EF(1%)s and two flexible queries (3IND, 3RTN), which resulted in adequate EF(1%) values were selected for investigation. First of all, the influence of pharmacophore atomic assignment was studied. Instead of ChemAxon's extended atom type assignment during initialization, pharmacophore atomic assignment was applied. The Shape algorithm was chosen and compared to those given by ChemAxon's extended atomic type assignation. We did not find significant differences in EF(1%) and BEDROC(20) values. It is worth noting that changing the default pharmacophore definition can significantly alter the alignments and influence the effectiveness of the shape similarity searches; however, that can be part of further studies. Second, the number of starting conformations was increased from two to five. It did not influence the results for Shape while it decreased the EF(1%)s and BEDROC(20) values for the Match method.

dx.doi.org/10.1021/ci400620f | J. Chem. Inf. Model. 2014, 54, 1036−1049

Finally, we modified the molecular alignment accuracy. We did not find any relevant influence on the EF(1%) or BEDROC(20) values either.

These calculations further support our previous finding that the default algorithm is robust and provides consistent results. It is interesting to note that exploring the imprecision of the scoring functions was not part of this study. Their inability to capture the fine differences between the various alignment methods could be a possible reason for finding no relevant additional parameters that influenced the screening performance. These calculations could be worth exploring by computational experts.[10]

Comparative Virtual Screening. In this subsection without the need of completeness we discuss several state-of-the-art virtual screening methods in contrast to Screen3D.

2D Similarity Studies. Fingerprint-based similarity searches were run by the Screen2D program package on DUD and DUD-E data sets. ECFP6 and pharmacophore fingerprints (Pharm-Calc) calculations were performed constituting twenty−twenty runs (Figure 10). Queries 2VIJ and 3L5C provided the best results against the DUD screening data set (EF(1%) = 20, 3L5C, Pharm-Calc) while 2ZJM, 3IND, 3L38, 3L3A, 3LPI, 3MSK, 3RTN, and 3RVI presented very poor EF(1%) or BEDROC(20) values. The DUD-E data set implicated a larger challenge for the algorithm as EF(1%)s were worse than given for the DUD screening data set. It should be noted that both fingerprints showed similar results on both screening data sets, and the dependency of the effectiveness on the query structures was relevant while on the methods it was negligible.

Comparing the query structures that provided the best results by Screen2D to that of Screen3D suggests that different query structures provided best results for Screen2D and Screen3D. It reveals that these approaches can be rather complementary than competitive. A method overlap analysis was also performed; the first 2% (100 molecules) of the ranked databases were compared and the rate of identical actives was analyzed (see the Supporting Information). The analyses revealed that 2D similarity methods retrieved different structures from those found by Screen3D. Therefore these methods are not only complementary but could possibly be applied for scaffold hopping studies or fused data screens. In other words, 2D similarity often characterizes molecules differently, while 3D similarity recognizes similar shapes.

Docking Studies. Since docking calculations served as rough comparison points in terms of screening performance measured by EF(1%) and BEDROC(20) values, a substantial head-to-head comparison was not executed.

Six X-ray structures (2VIJ, 2ZJM, 3IND, 3L3A, 3L5C, 3RTN) and the DUD screening data set were selected for docking studies. Among the crystal structures both open and closed FLAP conformations were found. 10s loop exhibited various conformations; therefore, all relevant conformational classes were represented.[14] In our previous studies we showed the dependency of the results on ligand protonation and the protonation of the catalytic dyad.[24,25] Therefore according to our previous findings Asp32 was protonated and Asp298 was ionized, and all the molecules in the screening database were neutral.[25] It is important to note that docking studies largely depend on confounding factors; therefore, it is always advisable to optimize the docking protocol for a given problem.[62,63] This time we used the default settings to present its performance without its optimization. Numerous studies reported successful approaches for optimization through selection of best scoring functions, involvement of solvation or data fusion.[64−66] Protein flexibility was also omitted that usually can improve the effectiveness.[25,67,68]

Goldscore and CHEMPLP were applied as docking scores. Of the twenty active molecules only seventeen were docked, and of the 5000 molecules approximately 4500 were docked successfully for each of the six runs. CHEMPLP outperformed Goldscore and resulted in the best EF(1%) and BEDROC(20) values (Table 1). The best EF(1%) was 25 for 3L5C and 3RTN. The best hit rate was 5% (10/200).

Table 1. Summary of Docking Results Calculated by the Gold Algorithm for Six X-ray Structures on the DUD Screening Data Set

DUD EF (1%)	2VIJ	2ZJM	3IND	3L3A	3L5C	3RTN
GoldScore	5	0	0	0	15	10
CHEMPLP	20	0	10	10	25	25

Gold performance was comparable in terms of EF(1%) and BEDROC(20) values to Screen3D. In contrast to Screen3D Gold provided good results for 2VIJ and 3L5C structures; it suspects that docking studies can serve as a complement to shape-based similarity studies.

Comparison to Third Party Virtual Screening Tools. Ten popular ligand-based virtual screening tools using the publicly available DUD data set with more than 100 000 compounds for 40 protein targets was studied by Venkatraman[26] and co-workers. Although 3D molecular shape is an important determinant of biological activity, their results showed that the 2D fingerprint-based methods generally gave better virtual screening performance than the shape-based approaches for many of the DUD targets. They proposed to improve the performance of 3D methods, and it was necessary to devise screening queries that can represent multiple possible conformations and which can exploit knowledge of known actives that span multiple scaffold families.

Our results (Table 2) indicate that Screen3D performs similarly to popular ligand-based methods like Babel, Daylight, and BCI and significantly outperforms shape-based methods found in this publication. These results also highlight the importance of combined usage of 2D and 3D approaches because 2D similarity often retrieves different molecules than 3D similarity (see the Supporting Information for heatmap). However, the investigation of this particular question here was not part of our study because our intention was to give an overall performance comparison. Evaluating Screen3D highlights similar EF(1%) and AUC(100%) values, independently on the method, the score and query flexibility. It is worth noting that the performance of all VS methods significantly depends on the actual query and target library, resulting in substantially different rankings case by case. Here we only provide the mean values for comparison purposes. In the Supporting Information further data of the methods using EF(5%) EF(10%) with standard deviations included are given.

Giganti et al. published their comparative virtual screening study incorporating Surflex-Dock/Surflex-Sim, FlexX/FlexS, ICM, and OMEGA-FRED/OMEGA-ROCS. They investigated 11 systems from the challenging "own" subsets of the Directory of Useful Decoys (DUD-own); the performances of the programs above in terms of molecular alignment accuracy,

Table 2. EF(1%) and AUC(100%) Values Calculated on Venkatraman's Data Set by Screen3D and Compared to the Values Published by the Authors[26]

	methods	Score	EF (1%)	AUC (100%)
Query Flexible	Shape	Screen3D	19.3	0.73
		Tanimoto	18.7	0.70
	Match	Screen3D	19.5	0.73
		Tanimoto	18.7	0.70
Query Rigid	Shape	Screen3D	20.2	0.72
		Tanimoto	19.0	0.70
	Match	Screen3D	19.45	0.72
		Tanimoto	19.0	0.70
screening performance of various VS tools benchmarked by Venkatraman et al.		Babel	18.9	0.76
		Daylight	18.7	0.76
		MACCS	13.6	0.71
		BCI	19.6	0.76
		MOLPRINT2D	16.1	0.70
		PARAFIT_S	7.9	0.66
		ROCS_SC	15.5	0.70
		ROCS_S	10.6	0.63
		EON_SCE	10.9	0.68
		EON_SE	10.5	0.68
		SHAEP_SE	11.4	0.65
		SHAEP_S	11.2	0.65
		USR	5.3	0.60
		ESHAPE3D_HYD	6.7	0.50
		ESHAPE3D	7	0.44

enrichment in active compounds, and enrichment in different chemotypes (scaffold hopping) were evaluated and compared.

We demonstrated Screen3D performance in terms of EF(1%) values and compared them to Giganti's findings (Figure 11). Screen3D provided poor results on FXA; however, for the rest of the targets Screen3D outperformed or gave comparable results to both docking and shape-based screening methods. We also provided EF(10%) values in the Supporting Information.

These two studies revealed that Screen3D provides adequate results on a broad range of target proteins, and its performance is in the range of other methods. Since Screen3D implements a novel approach, it can find hit molecules different from ones found by other methods; however, this must be investigated in further studies. This was initially suggested by the method overlap study (Supporting Information).

Numerous further studies demonstrate that ligand-based virtual screening is competitive and often superior to structure-based methods. Hawkins et al. published a direct comparison between a number of docking programs and a shape-based ranking method (ROCS). In total, seven different docking programs were compared to ROCS across 21 different protein systems. ROCS provided superior performance even when a bioactive conformation of the ligand was not known for over half of the cases.[69] Authors discussed a frequent problem of shape-based methods, the problem of losing the false negative hits; active molecules with shape and size different from that of the query are often missed. Although shape similarity methods lose false negatives, they can retrieve novel chemistries within the shape classes. This observation raises the question: which molecule and conformation should be used as a query, and how should they be chosen. Screen3D, an easy-to-use tool that can be run on a single processor, allows even a non-expert to quickly execute shape similarity screens using several query structures reducing the false negative hits. However, our findings supported that shape-based and fingerprint-based searches with docking studies could lead to the best performance due to the complementary nature of these methods.[69,70]

Hamza et al. have developed a robust new scoring function (HWZ score) for the ligand-based (shape-filtering) virtual

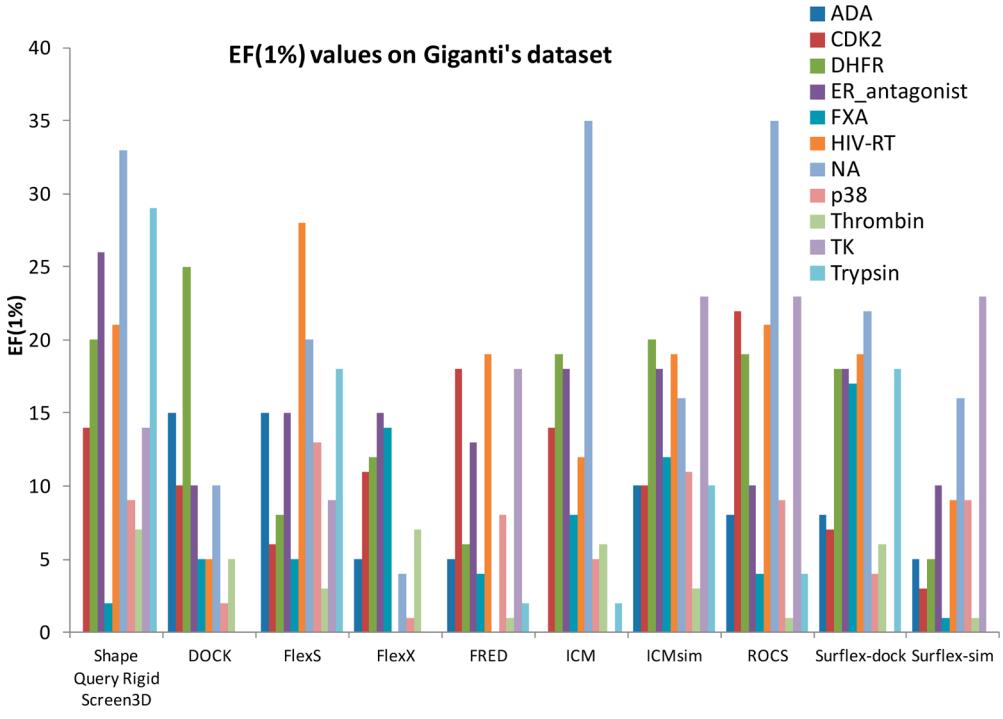

Figure 11. EF(1%) values calculated on Giganti's data set by Screen3D and results compared to the published values.[27]

dx.doi.org/10.1021/ci400620f | J. Chem. Inf. Model. 2014, 54, 1036−1049

screening method.[71] They compared popularly used shape-filtering virtual screening approaches and different scoring functions. 40 protein targets in the DUD database were part of their examinations where the HWZ score-based virtual screening approach led to an improved overall performance based on the obtained AUC (area under the curve), enrichment factor, and hit rate values. In addition, the performance of the HWZ score-based virtual screening approach was less sensitive to the choice of the target. The generation of a novel and robust scoring function is useful not only for ligand-based virtual screening algorithms but also for docking studies. According to our findings the performance of Screen3D showed dependency on its two built-in scores; moreover this dependency was inconsistent. Further explorative studies using more scoring functions could provide a deeper understanding of inconsistency. Furthermore, the Screen3D algorithm could provide improved performance and consistency with robust scoring functions.

Phase Shape, another widely used shape-based search method developed by Schrödinger Inc., was shown to rapidly produce accurate 3D ligand alignments and efficiently enrich actives in virtual screening. This methodology is based on the principle of atom distribution triplets that rapidly defines trial alignments and serves as a starting point for further refinements to maximize the volume overlap. The method can be run in a shape-only mode or it can include atom types or pharmacophore feature encoding. The latter consistently produces the best results for database screening. Phase Shape allows the application of multiple parameters including atom typing, query structure conformation, and the database conformer generation protocol.[72] Although phase Shape was shown to be a robust method that is slightly dependent on several parameters including the initial query conformation, along with the number of conformation and generated diverse hits it also suffers from the limitation of other shape-based search methods like missing false negative hits due to the inability of a single query conformation to retrieve all the actives. Sastry et al.[73] used three different virtual screening methods (two-dimensional (2D) fingerprint similarity, shape-based similarity (Phase Shape), and docking) on two different databases (DUD and MDDR) to show that combining results from multiple methods using a standard score (Z-score) can significantly improve virtual screening enrichments reducing false negatives. Since Screen3D allows a fully flexible and very fast search method, the execution of several shape-based screens can be accomplished even on an average home computer. Our findings were also similar to that of Sastry et al. in terms of combining the results of multiple query structures to achieve a more diverse and higher hit rate, slight dependency on several parameters.[73−76]

Computational Environment and Running Times. Screen2D was used as downloadable in the JChem 6.2 program package, and Screen3D was from the 6.3 development version. All 2D and 3D calculations were run on Intel(R) Xeon(R) E31230@3.20 GHz processors with 8 GB RAM. The Screen3D calculations for rigid-flexible overlays were performed on 8 parallel threads resulting in an average runtime of 80 ms/molecule pair comparison and a median runtime of 54 ms/molecule pair comparison.

Screen2D fingerprint similarity searches take an average of about 5 s for 5000 molecules. Docking calculations take about 250 s per ligand including the generation of conformations and scoring. Based on these observations Screen3D and Screen2D can be used as desktop tools on even laptops, while docking needs more computational power that allows even non-computational experts to execute searches.

CONCLUSION

Ligand-based virtual screening (LBVS) is to identify bioactive ligands through computational means by employing knowledge about known bioactive ligands. In LBVS, a large number of molecules are ranked according to their likelihood to be bioactive compounds. In choosing the right approach, the researcher is faced with many questions: where is the optimum between efficiency and accuracy when evaluating a particular algorithm; in which situations does some method perform better than others. Given the multitude of settings, parameters, and data sets the practitioner can choose from, there are many pitfalls that lurk along the way which might ruin the final output.

In this paper we presented a novel algorithm, Screen3D, that offers a robust way to execute routine calculations for even non-experts and can also facilitate the communication between experts and non-experts. Screen3D can prevent users from parameter optimization and the deep understanding of chemoinformatics. The flexibility of the algorithm is kept; therefore, it offers several parameters for expert users. The screening performance was found to be more dependent on the query structures and not on the actual method or parameter set. Application of single query structures lead to high false negative rates; however, Screen3D offers a fast and easy execution for multiple query searches ensuring a broader structural coverage in the hit lists. However, the thorough knowledge of the target biology and the deep understanding of the protein−ligand interaction cannot be avoided even for non-experts.

On average Screen3D performed similarly to 2D fingerprint-based methods evaluated in this study; moreover it returns significantly different hits. This makes Screen3D a valuable tool for scaffold hopping or descriptor data fusion scenarios.

Screen3D offers numerous ways for shape-based similarity screening alone or in combination with other methods. Since it is a desktop application, available in Knime workflow tool, we suggest this algorithm for even larger scale routine searches to any pharmaceutical scientists.

ASSOCIATED CONTENT

Supporting Information

Screen3D and Screen2D calculations, BACE1-DUD data set, EF(1%), and BEDROC(20) values with various options; various setups applied for Screen3D calculations; setups for Screen3D additional option evaluation; summary of Screen2D runs; dissimilarity distribution between actives and inactives for BACE1-DUD and BACE1-DUD-E data sets; method overlap; comparison results on DUD Release data set; comparison results on the DUD data set − subset of 11 protein targets; enrichment values of the VS tools. This material is available free of charge via the Internet at http://pubs.acs.org.

AUTHOR INFORMATION

Corresponding Authors

*E-mail: akalaszi@chemaxon.com (A.K.).
*E-mail: timea.polgar@gmail.com (T.P.).

Notes

The authors declare no competing financial interest.

■ ACKNOWLEDGMENTS

The authors are thankful to Christopher Southan (IUPHAR Database and Guide to Pharmacology web portal) and Jason Cole (Cambridge Crystallographic Data Centre) for reviewing the manuscript and for their valuable suggestions. We thank our colleagues Ödön Farkas, Miklós Vargyas, and Miklós J. Szabó for their stimulating ideas and fruitful conversations.

■ REFERENCES

(1) Klebe, G. Virtual ligand screening: strategies, perspectives and limitations. *Drug Discovery Today* **2006**, *11*, 580−94.
(2) Polgar, T.; Keseru, G. M. In *Encyclopedia of Pharmaceutical Technology*, 3rd ed.; Taylor&Francis: 2013; pp 4013−4038.
(3) Alvarez, J.; Shoichet, B. *Virtual Screening in Drug Discovery*; Taylor&Francis: 2005.
(4) Geppert, H.; Vogt, M.; Bajorath, J. Current Trends in Ligand-Based Virtual Screening: Molecular Representations, Data Mining Methods, New Application Areas, and Performance Evaluation. *J. Chem. Inf. Model.* **2010**, *50*, 205−216.
(5) Willet, P. In *Chemoinformatics and Computational Chemical Biology, Methods in Molecular Biology*; Springer: 2011; Vol. *672*, pp 133−158.
(6) Duan, J.; Dixona, S. L.; Lowriea, J. F.; Sherman, W. Analysis and comparison of 2D fingerprints: Insights into database screening performance using eight fingerprint methods. *J. Mol. Graphics Modell.* **2010**, *29*, 157−170.
(7) Ehrlich, H.-C.; Rarey, M. Maximum common subgraph isomorphism algorithms and their applications in molecular science: A review. *WIREs Comput. Mol. Sci.* **2011**, *1*, 68−79.
(8) Vogt, M.; Bajorath, M. *Chemoinformatics and Computational Chemical Biology: Predicting the Performance of Fingerprint Similarity Searching*; Springer: 2011; Vol. *672*, pp 159−173.
(9) Mcgaughey, G. B.; Sheridan, R. P.; Bayly, C. I.; Culberson, J. C.; Kreatsoulas, C.; Lindsley, S.; Maiorov, V.; Truchon, J.; Cornell, W. D. Comparison of topological, shape, and docking methods in virtual screening. *J. Chem. Inf. Model.* **2007**, *47*, 1504−1519.
(10) Hamza, A.; Wei, N.-N.; Zhan, C.-G. Ligand-based virtual screening approach using a new scoring function. *J. Chem. Inf. Model.* **2012**, *52*, 963−74.
(11) Meslamani, J.; Li, J.; Sutter, J.; Stevens, A.; Bertrand, H.; Rognan, D. Protein-ligand-based pharmacophores: generation and utility assessment in computational ligand profiling. *J. Chem. Inf. Model.* **2012**, *52*, 943−955.
(12) Sastry, M.; Lowrie, J. F.; Dixon, S. L.; Sherman, W. Large-scale systematic analysis of 2D fingerprint methods and parameters to improve virtual screening enrichments. *J. Chem. Inf. Model.* **2010**, *50*, 771−784.
(13) Ebalunode, J. O.; Zheng, W. Unconventional 2D shape similarity method affords comparable enrichment as a 3D Shape algorithm in virtual screening experiments. *J. Chem. Inf. Model.* **2009**, *49*, 1313−20.
(14) Polgar, T.; Keseru, G. M. In *Current Pharmaceutical Design*; Bentham Science Publishers: 2013.
(15) Kirchmair, J.; Ristic, S.; Eder, K.; Markt, P.; Wolber, G.; Laggner, C.; Langer, T. Fast and efficient in-silico 3D screening: Towards maximum computational efficiency of pharmacophore-based and shape-based approaches. *J. Chem. Inf. Model.* **2007**, *47*, 2182−96.
(16) Hawkins, P. C. D.; Skillman, G.; Nicholls, A. Comparison of shape-matching and docking as virtual screening tools. *J. Med. Chem.* **2007**, *50*, 74−82.
(17) Nicholls, A.; McGaughey, G. B.; Sheridan, R. P.; Good, A. C.; Warren, G.; Mathieu, M.; Kelley, B. Molecular shape and medicinal chemistry: A perspective. *J. Med. Chem.* **2010**, *53*, 3862−3886.
(18) Hu, G.; Kuang, G.; Xiao, W.; Li, W.; Liu, G.; Tang, Y. Performance evaluation of 2D fingerprint and 3D shape similarity methods in virtual screening. *J. Chem. Inf. Model.* **2012**, *52*, 1103−1113.
(19) Bender, A.; Jenkins, J. L.; Scheiber, J.; Sukuru, S. C. K.; Glick, M.; Davies, J. W. How similar are similarity searching methods? A principal component analysis of molecular descriptor space. *J. Chem. Inf. Model.* **2009**, *49*, 108−119.
(20) Moffat, K.; Gillet, V. J.; Whittle, M.; Bravi, G.; Leach, A. R. A comparison of field-based similarity methods. *J. Chem. Inf. Model.* **2008**, *48*, 719−729.
(21) Grant, J. A.; Gallardo, M. A.; Pickup, B. A fast method of molecular shape comparison: A simple application of a Gaussian description of molecular shape. *J. Comput. Chem.* **1996**, *17*, 1653−1663.
(22) Lemmen, C.; Lengauer, T.; Klebe, G. FlexS: A method for fast flexible ligand superposition. *J. Med. Chem.* **1998**, *23*, 4502−4520.
(23) Sastry, G. M.; Dixon, S. L.; Sherman, W. Rapid shape-based ligand alignment and virtual screening method based on atom/feature-pair similarities and volume overlap scoring. *J. Chem. Inf. Model.* **2011**, *51*, 2455−2466.
(24) Polgár, T.; Keseru, G. M. Virtual screening for β-secretase (BACE1) inhibitors reveals the importance of protonation states at Asp32 and Asp228. *J. Med. Chem.* **2005**, *48*, 3749−3755.
(25) Polgár, T.; Keseru, G. M. Ensemble docking into flexible active sites. Critical evaluation of FlexE against JNK-3 and β-secretase. *J. Chem. Inf. Model.* **2006**, *46*, 1795−1805.
(26) Venkatraman, V.; Perez-Nueno, V. I.; Mavridis, L.; Ritchie, D. W. Comprehensive comparison of ligand-based virtual screening tools against the DUD data set reveals limitations of current 3D methods. *J. Chem. Inf. Model.* **2010**, *50*, 2079−2093.
(27) Giganti, D.; Guillemain, H.; Spadoni, J. L.; Nilges, M.; Zagury, J. F.; Montes, M. Comparative evaluation of 3D virtual ligand screening methods: impact of the molecular alignment on enrichment. *J. Chem. Inf. Model* **2010**, *50*, 992−1004.
(28) Truchon, J. F.; Bayly, C. I. Evaluating virtual screening methods: good and bad metrics for the "early recognition" problem. *J. Chem. Inf. Model.* **2007**, *47*, 488−508.
(29) ChemAxon Software, www.chemaxon.com, 2014.
(30) Mayo, S. L.; Olafson, B. D.; Goddard, W. A. DREIDING: A generic force field for molecular simulations. *J. Phys. Chem.* **1990**, *94*, 8897−8909.
(31) Farkas, Ö.; Schlegel, B. H. Geometry optimization methods for modeling large molecules. *J. Mol. Struct.: THEOCHEM* **2003**, *666*, 31−39.
(32) Hurst, T. Flexible 3D searching: The directed tweak technique. *J. Chem. Inf. Comput. Sci.* **1994**, *34*, 190−196.
(33) Karney, C. F. Quaternions in molecular modeling. *J. Mol. Graphics Modell.* **2007**, *25*, 595−604.
(34) Good, A. C.; Richards, W. G. Rapid evaluation of shape similarity using Gaussian functions. *J. Chem. Inf. Comput. Sci.* **1993**, *33*, 112−116.
(35) Dodd, L. R.; Theodoru, D. N. Analytical treatment of the volume and surface area of molecules formed by an arbitrary collection of unequal spheres intersected by planes. *Mol. Phys.* **1991**, *72*, 1313−1345.
(36) Huang, N.; Shoichet, B. K.; Irwin, J. J. Benchmarking sets for molecular docking. *J. Med. Chem.* **2006**, *49*, 6789−6801.
(37) Von Korff, M.; Freyss, J.; Sander, T. Comparison of ligand- and structure-based virtual screening on the DUD data set. *J. Chem. Inf. Model.* **2009**, *49*, 209−31.
(38) Mysinger, M. M.; Carchia, M.; Irwin, J. J.; Shoichet, B. K. Directory of useful decoys, enhanced (DUD-E): better ligands and decoys for better benchmarking. *J. Med. Chem.* **2012**, *55*, 6582−94.
(39) Mandal, M.; Zhu, Z.; Cumming, J. N.; Liu, X.; Strickland, C.; Mazzola, R. D.; Caldwell, J. P.; Leach, P.; Grzelak, M.; Hyde, L.; Zhang, Q.; Terracina, G.; Zhang, L.; Chen, X.; Kuvelkar, R.; Kennedy, M. E.; Favreau, L.; Cox, K.; Orth, P.; Buevich, A.; Voigt, J.; Wang, H.; Kazakevich, I.; McKittrick, B. A.; Greenlee, W.; Parker, E. M.; Stamford, A. W. Design and validation of bicyclic iminopyrimidinones as beta amyloid cleaving enzyme-1 (BACE1) inhibitors: Conformational constraint to favor a bioactive conformation. *J. Med. Chem.* **2012**, *55*, 9331−9345.

(40) Malamas, M. S.; Erdei, J.; Gunawan, I.; Turner, J.; Hu, Y.; Wagner, E.; Fan, K.; Chopra, R.; Olland, A.; Bard, J.; Jacobsen, S.; Magolda, R. L.; Pangalos, M.; Robichaud, A. J. Design and synthesis of 5,5′-disubstituted aminohydantoins as potent and selective human beta-secretase (BACE1) inhibitors. *J. Med. Chem.* **2010**, *53*, 1146−1158.
(41) Madden, J.; Dod, J. R.; Godemann, R.; Kraemer, J.; Smith, M.; Biniszkiewicz, M.; Hallett, D. J.; Barker, J.; Dyekjaer, J. D.; Hesterkamp, T. Fragment-based discovery and optimization of BACE1 inhibitors. *Bioorg. Med. Chem. Lett.* **2010**, *20*, 5329−5333.
(42) Rosbrook, G. O.; Stead, M. A.; Carr, S. B.; Wright, S. C. The structure of the Bach2 POZ-domain dimer reveals an intersubunit disulfide bond. *Acta Crystallogr., Sect. D* **2012**, *68*, 26−34.
(43) Cheng, Y.; Judd, T. C.; Bartberger, M. D.; Brown, J.; Chen, K.; Fremeau, R. T.; Hickman, D.; Hitchcock, S. A.; Jordan, B.; Li, V.; Lopez, P.; Louie, S. W.; Luo, Y.; Michelsen, K.; Nixey, T.; Powers, T. S.; Rattan, C.; Sickmier, E. A.; St Jean, D. J.; Wahl, R. C.; Wen, P. H.; Wood, S. From fragment screening to in vivo efficacy: optimization of a series of 2-aminoquinolines as potent inhibitors of beta-site amyloid precursor protein cleaving enzyme 1 (BACE1). *J. Med. Chem.* **2011**, *54*, 5836−5857.
(44) Banner, D. W.; Gsell, B.; Benz, J.; Bertschinger, J.; Burger, D.; Brack, S.; Cuppuleri, S.; Debulpaep, M.; Gast, A.; Grabulovski, D.; Hennig, M.; Hilpert, H.; Huber, W.; Kuglstatter, A.; Kusznir, E.; Laeremans, T.; Matile, H.; Miscenic, C.; Rufer, A.; Schlatter, D.; Steyeart, J.; Stihle, M.; Thoma, R.; Weber, M.; Ruf, A. Mapping the conformational space accessible to Bace2 using surface mutants and co-crystals with fab-fragments, fynomers, and xaperones. *Acta Crystallogr., Sect. D* **2013**, *69*, 1124.
(45) Bowers, S.; Xu, Y. Z.; Yuan, S.; Probst, G. D.; Hom, R. K.; Chan, W.; Konradi, A. W.; Sham, H. L.; Zhu, Y. L.; Beroza, P.; Pan, H.; Brecht, E.; Yao, N.; Lougheed, J.; Tam, D.; Ren, Z.; Ruslim, L.; Bova, M. P.; Artis, D. R. Structure-based design of novel dihydroisoquinoline BACE-1 inhibitors that do not engage the catalytic aspartates. *Bioorg. Med. Chem. Lett.* **2013**, *23*, 2181−2186.
(46) Swahn, B.; Holenz, J.; Kihlstrom, J.; Kolmodin, K.; Lindstrom, J.; Plobeck, N.; Rotticci, D.; Sehgelmeble, F.; Sundstrom, M.; Vonberg, S.; Falting, J.; Georgievska, B.; Gustavsson, S.; Neelissen, J.; Ek, M.; Olsson, L. L.; Berg, S. Aminoimidazoles as Bace-1 inhibitors: The challenge to achieve in vivo brain efficacy. *Bioorg. Med. Chem. Lett.* **2012**, *22*, 1854−1866.
(47) Swahn, B. M.; Kolmodin, K.; Karlstrom, S.; Von Berg, S.; Soderman, P.; Holenz, J.; Berg, S.; Lindstrom, J.; Sundstrom, M.; Turek, D.; Kihlstrom, J.; Slivo, C.; Andersson, L.; Pyring, D.; Rotticci, D.; Ohberg, L.; Kers, A.; Bogar, K.; Von Kieseritzky, F.; Bergh, M.; Olsson, L. L.; Janson, J.; Eketjall, S.; Georgievska, B.; Jeppsson, F.; Falting, J. Design and synthesis of beta-site amyloid precursor protein cleaving enzyme (BACE1) inhibitors with in vivo brain reduction of beta-amyloid peptides. *J. Med. Chem.* **2012**, *55*, 9346.
(48) Rueeger, H.; Rondeau, J. M.; McCarthy, C.; Mobitz, H.; Tintelnot-Blomley, M.; Neumann, U.; Desrayaud, S. Structure based design, synthesis and SAR of cyclic hydroxyethylamine (HEA) BACE-1 inhibitors. *Bioorg. Med. Chem. Lett.* **2011**, *21*, 1942−1947.
(49) Kaller, M. R.; Harried, S. H.; Albrecht, B.; Amarante, P.; Babu-Khan, S.; Bartberger, M. D.; Brown, J.; Brown, R.; Chen, K.; Cheng, Y.; Citron, M.; Croghan, M. D.; Dunn, R.; Graceffa, R.; Hickman, D.; Judd, T.; Kriemen, C.; La, D.; Lopez, P.; Luo, Y.; Masse, C.; Monenschein, H.; Nguyen, T.; Pennington, L. D.; Miguel, T. S.; Sickmier, E. A.; Wahl, R. C.; Weiss, M.; Wen, P. H.; Williamson, T.; Wood, S.; Xue, M.; Yang, B.; Zhang, J.; Patel, V.; Zhong, W.; Hitchcock, S. A potent and orally efficacious, hydroxyethylamine-based inhibitor of beta-secretase. *ACS Med. Chem. Lett.* **2012**, *3*, 886−891.
(50) Polgár, T.; Magyar, C.; Simon, I.; Keserü, G. M. Impact of ligand protonation on virtual screening against β-secretase (BACE1). *J. Chem. Inf. Model.* **2007**, *47*, 2366−2373 (2007).
(51) Barrow, J. C.; Stauffer, S. R.; Rittle, K. E.; Ngo, P. L.; Yang, M. S.; Graham, S.; McGaughey, G.; Holloway, K.; Tugusheva, S. K.; Lai, M.; Espeseth, A. S.; Xu, M.; Huang, Q.; Zuck, P.; Levorse, D. A.; Hazuda, D.; Vacca, J. P. Discovery and X-ray crystallographic analysis of a spiropiperidine iminohydantoin inhibitor of beta-secretase. *J. Med. Chem.* **2008**, *51*, 6259−6262.
(52) Hanessian, S.; Shao, Z.; Betschart, C.; Rondeau, J. M.; Neumann, U.; Tintelnot-Blomley, M. Structure-based design and synthesis of novel P2/P3 modified, non-peptidic beta-secretase (BACE-1) inhibitors. *Bioorg. Med. Chem. Lett.* **2010**, *20*, 1924−1927.
(53) Rueeger, H.; Lueoend, R.; Rogel, O.; Rondeau, J. M.; Mobitz, H.; Machauer, R.; Jacobson, L.; Staufenbiel, M.; Desrayaud, S.; Neumann, U. Discovery of cyclic sulfone hydroxyethylamines as potent and selective β-site APP-cleaving enzyme 1 (BACE1) inhibitors: structure-based design and in vivo reduction of amyloid β-peptides. *J. Med. Chem.* **2012**, *55*, 3364−3386.
(54) Sealy, J. M.; Truong, A. P.; Tso, L.; Probst, G. D.; Aquino, J.; Hom, R. K.; Jagodzinska, B. M.; Dressen, D.; Wone, D. W.; Brogley, L.; John, V.; Tung, J. S.; Pleiss, M. A.; Tucker, J. A.; Konradi, A. W.; Dappen, M. S.; Toth, G.; Pan, H.; Ruslim, L.; Miller, J.; Bova, M. P.; Sinha, S.; Quinn, K. P.; Sauer, J. M. Design and synthesis of cell potent BACE-1 inhibitors: structure-activity relationship of P1′ substituents. *Bioorg. Med. Chem. Lett.* **2009**, *19*, 6386−6391.
(55) Beswick, P.; Charrier, N.; Clarke, B.; Demont, E.; Dingwall, C.; Dunsdon, R.; Faller, A.; Gleave, R.; Hawkins, J.; Hussain, I.; Johnson, C. N.; MacPherson, D.; Maile, G.; Matico, R.; Milner, P.; Mosley, J.; Naylor, A.; O'Brien, A.; Redshaw, S.; Riddell, D.; Rowland, P.; Skidmore, J.; Soleil, V.; Smith, K. J.; Stanway, S.; Stemp, G.; Stuart, A.; Sweitzer, S.; Theobald, P.; Vesey, D.; Walter, D. S.; Ward, J.; Wayne, G. BACE-1 inhibitors part 3: identification of hydroxy ethylamines (HEAs) with nanomolar potency in cells. *Bioorg. Med. Chem. Lett.* **2008**, *18*, 1022−1026.
(56) Malamas, M. S.; Erdei, J.; Gunawan, I.; Turner, J.; Hu, Y.; Wagner, E.; Fan, K.; Chopra, R.; Olland, A.; Bard, J.; Jacobsen, S.; Magolda, R. L.; Pangalos, M.; Robichaud, A. J. Design and synthesis of 5, 5′-disubstituted aminohydantoins as potent and selective human β-secretase (BACE1) inhibitors. *J. Med. Chem.* **2009**, *53*, 1146−1158.
(57) Malamas, M. S.; Barnes, K.; Hui, Y.; Johnson, M.; Lovering, F.; Condon, J.; Fobare, W.; Solvibile, W.; Turner, J.; Hu, Y.; Manas, E. S.; Fan, K.; Olland, A.; Chopra, R.; Bard, J.; Pangalos, M. N.; Reinhart, P.; Robichaud, A. J. Novel pyrrolyl 2-aminopyridines as potent and selective human beta-secretase (BACE1) inhibitors. *Bioorg. Med. Chem. Lett.* **2010**, *20*, 2068−2073.
(58) Zhu, Z.; Sun, Z. Y.; Ye, Y.; Voigt, J.; Strickland, C.; Smith, E. M.; Cumming, J.; Wang, L.; Wong, J.; Wang, Y. S.; Wyss, D. F.; Chen, X.; Kuvelkar, R.; Kennedy, M. E.; Favreau, L.; Parker, E.; McKittrick, B. A.; Stamford, A.; Czarniecki, M.; Greenlee, W.; Hunter, J. C. Discovery of cyclic acylguanidines as highly potent and selective beta-site amyloid cleaving enzyme (BACE) inhibitors: Part I-inhibitor design and validation. *J. Med. Chem.* **2010**, *53*, 951−965.
(59) Cumming, J.; Babu, S.; Huang, Y.; Carrol, C.; Chen, X.; Favreau, L.; Greenlee, W.; Guo, T.; Kennedy, M.; Kuvelkar, R.; Le, T.; Li, G.; McHugh, N.; Orth, P.; Ozgur, L.; Parker, E.; Saionz, K.; Stamford, A.; Strickland, C.; Tadesse, D.; Voigt, J.; Zhang, L.; Zhang, Q. Piperazine sulfonamide BACE1 inhibitors: design, synthesis, and in vivo characterization. *Bioorg. Med. Chem. Lett.* **2010**, *20*, 2837−2842.
(60) Madden, J.; Dod, J. R.; Godemann, R.; Kraemer, J.; Smith, M.; Biniszkiewicz, M.; Hallett, D. J.; Barker, J.; Dyekjaer, J. D.; Hesterkamp, T. Fragment-based discovery and optimization of BACE1 inhibitors. *Bioorg. Med. Chem. Lett.* **2010**, *20*, 5329−5333.
(61) Cambridge Crystallographic Data Centre (CCDC), GOLD, http://www.ccdc.cam.ac.uk 2013.
(62) Warren, G. L.; Andrews, C. W.; Capelli, A.-M.; Clarke, B.; Lalonde, J.; Lambert, M. H.; Lindvall, L.; Nevins, N.; Semus, S. F.; Senger, S.; Tedesco, G.; Wall, I. D.; Woolven, J. M.; Peishoff, C. E.; Head, M. S. Critical assessment of docking programs and scoring functions. *J. Med. Chem.* **2006**, *49*, 5912−5931.
(63) Scior, T.; Bender, A.; Tresadern, G.; Medina-Franco, J. L.; Martínez-Mayorga, K.; Langer, T.; Agrafiotis, D. K. Recognizing pitfalls in virtual screening: a critical review. *J. Chem. Inf. Model.* **2012**, *52*, 867−881.

(64) Rastelli, G.; Rio, A. D.; Degliesposti, G.; Sgobba, M. Fast and accurate predictions of binding free energies using MM-PBSA and MM-GBSA. *J. Comput. Chem.* **2010**, *31*, 797−810.
(65) Willett, P. Combination of similarity rankings using data fusion. *J. Chem. Inf. Model.* **2013**, *53*, 1−10.
(66) Zhu, T.; Cao, S.; Su, P. C.; Patel, R.; Shah, D.; Chokshi, H. B.; Hevener, K. E. Hit identification and optimization in virtual screening: Practical recommendations based upon a critical literature analysis. *J. Med. Chem.* **2013**, DOI: 10.1021.
(67) Cosconati, S.; Marinelli, L.; Di Leva, F. S.; La Pietra, V.; De Simone, A.; Mancini, F.; Olson, A. J. Protein flexibility in virtual screening: the BACE-1 case study. *J. Chem. Inf. Model.* **2012**, *52*, 2697−2704.
(68) Hawkins, P. C. D.; Skillman, G.; Nicholls, A. Comparison of shape-matching and docking as virtual screening tools. *J. Med. Chem.* **2007**, *50*, 74−82.
(69) AbdulHameed, M. D. M.; Chaudhury, S.; Singh, N.; Sun, H.; Wallqvist, A.; Tawa, G. J. Exploring polypharmacology using a ROCS-based target fishing approach. *J. Chem. Inf. Model.* **2012**, *52*, 492−505.
(70) Hu, G.; Kuang, G.; Xiao, W.; Li, W.; Liu, G.; Tang, Y. Performance evaluation of 2D fingerprint and 3D shape similarity methods in virtual screening. *J. Chem. Inf. Model.* **2012**, *52*, 1103−1113.
(71) Hamza, A.; Wei, N. N.; Zhan, C. G. Ligand-based virtual screening approach using a new scoring function. *J. Chem. Inf. Model.* **2012**, *52*, 963−974.
(72) Sastry, G. M.; Inakollu, V. S. S.; Sherman, W. Boosting virtual screening enrichments with data fusion: Coalescing hits from 2D fingerprints, shape, and docking. *J. Chem. Inf. Model.* **2013**, *53*, 1531−1542.
(73) Meslamani, J.; Li, J.; Sutter, J.; Stevens, A.; Bertrand, H. O.; Rognan, D. Protein−ligand-based pharmacophores: generation and utility assessment in computational ligand profiling. *J. Chem. Inf. Model.* **2012**, *52*, 943−955.
(74) Watts, K. S.; Dalal, P.; Murphy, R. B.; Sherman, W.; Friesner, R. A.; Shelley, J. C. ConfGen: a conformational search method for efficient generation of bioactive conformers. *J. Chem. Inf. Model.* **2010**, *50*, 534−546.
(75) Spitzer, G. M.; Heiss, M.; Mangold, M.; Markt, P.; Kirchmair, J.; Wolber, G.; Liedl, K. R. One concept, three implementations of 3D pharmacophore-based virtual screening: distinct coverage of chemical search space. *J. Chem. Inf. Model.* **2010**, *50*, 1241−1247.
(76) Kirchmair, J.; Distinto, S.; Markt, P.; Schuster, D.; Spitzer, G. M.; Liedl, K. R.; Wolber, G. How to optimize shape-based virtual screening: choosing the right query and including chemical information. *J. Chem. Inf. Model.* **2009**, *49*, 678−692.